EDUCATUM JSMT Volume 11 Number 1 (2024)
ISSN 2289-7070 / e-ISSN 2462-2451(54-80)
https://ejournal.upsi.edu.my/index.php/EJSMT/index

Mathematical Modeling and Control Strategies for Nipah Virus Transmission Incorporating Bat-To-Pig-To-Human Pathway

Adedapo Chris Loyinmi[1], Sunday Oluwafemi Gbodogbe[2*]

[1,2]Department of Mathematics, Tai Solarin University of Education, Ogun State. Nigeria

[*]*Corresponding author:* sunspar06@gmail.com

Published: 17 January 2024

To cite this article (APA): Loyinmi, A. C., & Gbodogbe, S. O. (2024). Mathematical Modeling and Control Strategies for Nipah Virus Transmission Incorporating Bat-To-Pig-To-Human Pathway. *EDUCATUM Journal of Science, Mathematics and Technology*, *11*(1), 54–80. https://doi.org/10.37134/ejsmt.vol11.1.7.2024

To link to this article: https://doi.org/10.37134/ejsmt.vol11.1.7.2024

Abstract

The mathematical modeling of Nipah virus transmission, incorporating the bat-to-pig-to-human pathway, is essential for understanding this disease dynamics and optimizing control measures. Nipah virus, which naturally resides in animals, particularly fruit bats, spreads to humans via intermediate hosts like pigs. This research work highlights the significance of including this pathway in mathematical models for several crucial reasons. Firstly, it aids in comprehending zoonotic transmission, essential for designing effective control strategies. Secondly, it facilitates early detection and intervention by encompassing bats, pigs, and humans in the model. Monitoring factors such as bat population dynamics, pig infections, and human exposure enables timely intervention to prevent or mitigate outbreaks. Moreover, the complexity of Nipah virus transmission involving multiple species underscores the need for multifaceted control measures. We present a detailed mathematical model for Nipah virus transmission, including equations for human, pig, and bird populations. The model is rigorously analyzed, including the calculation of the basic reproduction number, the local stability of disease-free equilibrium, and the global stability of the equilibrium. Sensitivity analysis is performed to identify parameters with the most significant impact on disease dynamics. Optimal control strategies for the Nipah virus, incorporating personal prevention, treatment, biosecurity, and public health interventions, are developed and analyzed. Numerical simulations demonstrate the effectiveness of these control measures in reducing human and pig infections.
This research equips health practitioners with valuable insights and tools to better understand, prevent, and manage Nipah virus infections. Incorporating the bat-to-pig-to-human transmission pathway into mathematical models, provides a more holistic view of the disease's dynamics and enables health practitioners to implement more effective strategies for disease prevention and outbreak control.

Keywords: Nipah virus, Mathematical modeling, Bat-to-pig-to-human transmission, Control strategies, zoonotic transmission

INTRODUCTION

Nipah virus infection is a viral zoonotic ailment brought about by the Nipah virus (NiV), which belongs to the Henipavirus genus. The primary zoonotic host responsible for transmitting the virus to humans and animals, notably livestock such as pigs and horses, is fruit bats, also known as flying foxes. Nipah virus (NiV) derived its name from the Malaysian village where it was first identified in 1998 [1, 2, 3]. The initial outbreak had devastating consequences, with over 300 cases and 100 fatalities among pig farm workers in Malaysia and Singapore. Subsequently, nearly yearly outbreaks have been documented in Southeast Asia, with a particular focus on Bangladesh and eastern India [4, 5, 6]. As of February 2023, this year has already witnessed 10 reported cases, resulting in 7 tragic deaths in Bangladesh and this marks the sixth outbreak of Nipah virus in India since the initial report in 2001, which occurred in Siliguri town, West Bengal, resulting

in 66 cases and a case fatality rate (CFR) of 68% [1, 7, 8, 9]. Subsequently, five more outbreaks have been recorded: one in Nadia district, West Bengal (5 cases, CFR: 100%), another in Kozhikode and Malappuram, Kerala, in 2018 (comprising 23 cases, including confirmed and probable, with a CFR of 91%). In 2019, an isolated case was reported in Ernakulum, Kerala, and the patient survived. Then, in 2021, one case was documented in Kozhikode, Kerala, with a CFR of 100% [8, 10, 11, 12].

The virus can be transmitted to humans through the consumption of raw date palm sap and fruit that has been contaminated with secretions from bats, including saliva and urine. Additionally, transmission can occur through close contact with an infected animal or its bodily fluids. In the event of an infection, person-to-person transmission is possible, typically through close contact and via nasal and respiratory secretions, blood, and urine [11, 13, 14]. This type of transmission most commonly occurs within healthcare settings or among caregivers of individuals infected with NiV. It is worth noting that patients exhibiting respiratory symptoms are more likely to facilitate the spread of NiV.

Nipah Virus (NiV) infection can result in a spectrum of illness, spanning from mild to severe, which may include conditions such as encephalitis, and in some cases, it can be fatal. During the outbreak in Malaysia and Singapore, Nipah virus infection was linked to close contact with pigs infected with the virus [8, 14, 15, 16]. In contrast, in regions like Bangladesh and India, where Nipah virus infection is more prevalent, exposure has been associated with the consumption of raw date palm sap and contact with bats. It's worth noting that human-to-human transmission has been documented in these areas, and exposure to other individuals infected with Nipah virus is also considered a risk factor for contracting the disease [1, 18].

Diagnosing a patient with a clinical history of Nipah virus (NiV) infection involves a combination of tests during both the acute and convalescent phases of the disease. In the early stages, it is crucial to attempt virus isolation and conduct real-time polymerase chain reaction (RT-PCR) from throat and nasal swabs, cerebrospinal fluid, urine, and blood [17, 18, 19]. As the infection progresses, the use of antibody detection through enzyme-linked immunosorbent assay (ELISA) for both immunoglobulin G (IgG) and immunoglobulin M (IgM) can be valuable in confirming the diagnosis [18, 19, 20]. In cases where the disease results in a fatality, confirming the diagnosis may require immunohistochemistry on tissues collected during an autopsy, as this may be the only available method to establish the presence of the virus [14, 21, 22]. The treatment of Nipah virus infection primarily involves supportive care, as there is currently no specific antiviral medication available. Due to the potential for person-to-person transmission, adhering to standard infection control practices and employing proper barrier nursing techniques are vital in preventing hospital-acquired infections (nosocomial transmission) [18, 23]. Although the drug ribavirin has demonstrated effectiveness against the virus in laboratory settings, its clinical usefulness in human investigations remains uncertain and inconclusive [11]. Passive immunization, utilizing a human monoclonal antibody that targets the Nipah G glycoprotein, has shown benefits in post-exposure therapy in the ferret model [18, 24, 25].

To prevent Nipah virus infection, individuals should avoid contact with sick pigs and bats in endemic areas and refrain from consuming raw date palm sap. Enhanced surveillance and increased awareness are essential to prevent future outbreaks. Research efforts should focus on gaining a better understanding of the ecology of bats and Nipah virus, including exploring questions related to the seasonality of disease within the reproductive cycles of bats. Reliable laboratory assays for early disease detection in communities and livestock should be developed, and raising awareness about transmission and symptoms is crucial in reinforcing standard infection control practices, especially in healthcare settings to prevent human-to-human infections (nosocomial). A promising subunit vaccine that uses the Hendra G protein, which produces cross-protective antibodies against both Hendra virus and Nipah virus, has been employed in Australia to safeguard horses against Hendra virus. This vaccine holds significant potential for providing protection against henipaviruses in humans as well [18, 25, 26, 27, 28].

Mathematical modeling is a valuable tool for understanding the transmission dynamics of Nipah virus, predicting outbreaks, optimizing control strategies, allocating resources effectively, and guiding research and public health efforts [29, 30, 31]. These models play a crucial role in the proactive management of Nipah virus and other infectious diseases, ultimately helping to save lives and reduce the impact of outbreaks [32, 33, 34, 35, 36]. Numerous researchers have delved into the pathology and epidemiology of Nipah virus disease, yet only a limited number of models have been developed, as outlined below. Biswas, for instance, examined the disease dynamics using a foundational SIR mathematical model [37]. He proceeded to delve deeper into this model, exploring potential control and prevention strategies through

optimal control measures [37, 38]. Another SIR model also underwent optimization through the use of optimal control [39, 40]. Mondal et al. introduced a novel SEIR model designed to explore disease dynamics by incorporating two control parameters - the number of quarantined individuals and enhanced personal hygiene. These parameters had not been previously integrated into any Nipah virus dynamic model [41]. Shah et al. put forth an SEI model that takes into account the transmission of the disease from bats to humans and among humans. Furthermore, it considered a mode of disease transmission that hadn't been previously addressed - the transmission from human to human through unprotected contact with the deceased body of an individual infected with Nipah virus [42]. Durgesh et al., in their work [43], proposed an SVEIR model by considering interactions between bats and humans. They also delved into the role of vaccination in controlling the disease's spread. Lastly, Nita et al. introduced an SEIHD epidemic model with bat-human interaction [44], incorporating control measures such as insecticide spraying, bat burial, self-prevention, and hospitalization. Their research also delved into the dynamics of the disease and optimal control measures.

However, few or no research works incorporate bat-to-pig-to-human transmission pathway in mathematical modeling of Nipah virus which is crucial for several reasons. Firstly, it aids in comprehending zoonotic transmission, as Nipah virus naturally resides in animals, particularly fruit bats, and spreads to humans via intermediate hosts like pigs. This understanding is essential for designing effective control strategies. Secondly, it facilitates early detection and intervention by encompassing bats, pigs, and humans in the model. Monitoring factors such as bat population dynamics, pig infections, and human exposure enables timely intervention to prevent or mitigate outbreaks. Furthermore, the complexity of Nipah virus transmission, involving multiple species, underscores the need for multifaceted control measures. Mathematical models can assess the effectiveness of various strategies, including culling infected pigs, reducing bat-pig contact, enhancing biosecurity on pig farms, and implementing vaccination programs, all of which can significantly reduce the risk of human Nipah virus infections. Additionally, models considering multiple transmission pathways assist in the efficient allocation of limited resources, enabling decision-makers to target interventions where they are most needed based on the dynamics of bat-to-pig and pig-to-human transmission. Lastly, by comprehensively studying the bat-to-pig-to-human pathway, models can guide strategies to reduce the spillover of the virus from its natural reservoir (bats) to humans, which is key to reducing the overall burden of Nipah virus. In summary, the inclusion of the bat-to-pig-to-human transmission pathway in mathematical modeling of Nipah virus is essential for gaining a deeper understanding of disease dynamics and optimizing control measures. This approach promotes more effective disease prevention and outbreak management, ultimately reducing the risk of Nipah virus infections in humans and this is the significant of this study.

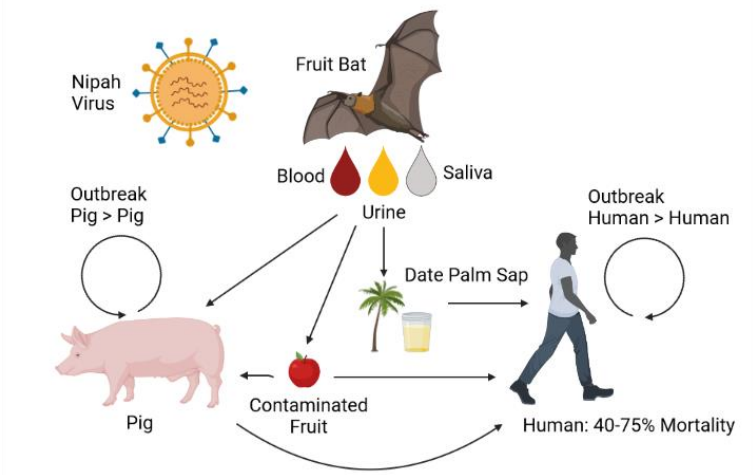

Figure 1: *Nipah Virus Transmission and Mortality*

MATERIALS AND METHODS

Model Formulation

This current framework for the transmission of monkeypox involves a total population that is divided into three distinct groups: N_H for humans, N_P for pigs, and N_B for birds.

N_H, which represents the human population, is further categorized into subgroups based on individuals' infection status within the population. These subgroups include those susceptible to the Nipah Virus (S_H), individuals who have been infected I_H, those under treatment to prevent further spread (T_H), and those who have recovered (R_H) from the infection.

N_P represents the pig population and is also subdivided into four categories: susceptible pigs (S_P) not infected with the Nipah virus, infected pigs (I_P), Nipah virus-infected pigs undergoing treatment (T_P), and pigs that have recovered from the virus (R_P).

N_B represents the bird population and is divided into two compartments: susceptible birds that have not been infected by the virus (S_B) and infected birds (I_B) that carry the Nipah virus.

This division enables us to study the disease dynamics separately within these three primary groups and also assists in analyzing the interactions and transmission dynamics of the Nipah Virus among humans, pigs, and birds. This approach offers a clearer understanding of how the disease spreads and allows for an examination of the impact of various control measures on human-to-human, pigs-to-human, pigs-to-pigs, birds-to-pigs, and birds-to-human transmission. The insights gained from this model can be valuable in developing effective strategies to manage and control Nipah virus outbreaks.

The force of Nipah virus infection is denoted as

$$\xi_B = \lambda_B\left(\frac{\phi_B I_B}{N_B}\right); \xi_P = \lambda_P\left(\frac{\phi_B I_B + \phi_P I_P}{N_P}\right); \xi_H = \lambda_H\left(\frac{\phi_B I_B + \phi_P I_P + \phi_H I_H}{N_H}\right) \quad (1)$$

Detailed parameters used in the model are described in Table 1, and a schematic diagram of the Nipah virus is presented in Figure 1.

Table 1: *Description of parameters used in the model*

Parameters	***Description***
ψ_H	Inclusion rate into the human class
ψ_P	Inclusion rate into the pig population
ψ_B	Inclusion rate into the bird society
ϕ_H	Adjustment infections state of infected human
ϕ_P	Adjustment infections state of infected pigs
ϕ_B	Adjustment infections state of infected birds
γ_H	Treatment rate of infected human
γ_P	Treatment rate of infected pig
σ_H	Recovery rate of infected human
σ_P	Recovery rate of infected pig
α_H	Natural death rate of human class
α_P	Natural death rate of pig population
α_B	Natural death rate of bird society
α_H	Nipah virus induced rate of infected human class
α_P	Nipah virus induced rate of infected pig population
α_B	Nipah virus induced rate in bird society

λ_H	Transmission rate of human class
λ_P	Transmission rate of pig population
λ_B	Transmission rate of bird society

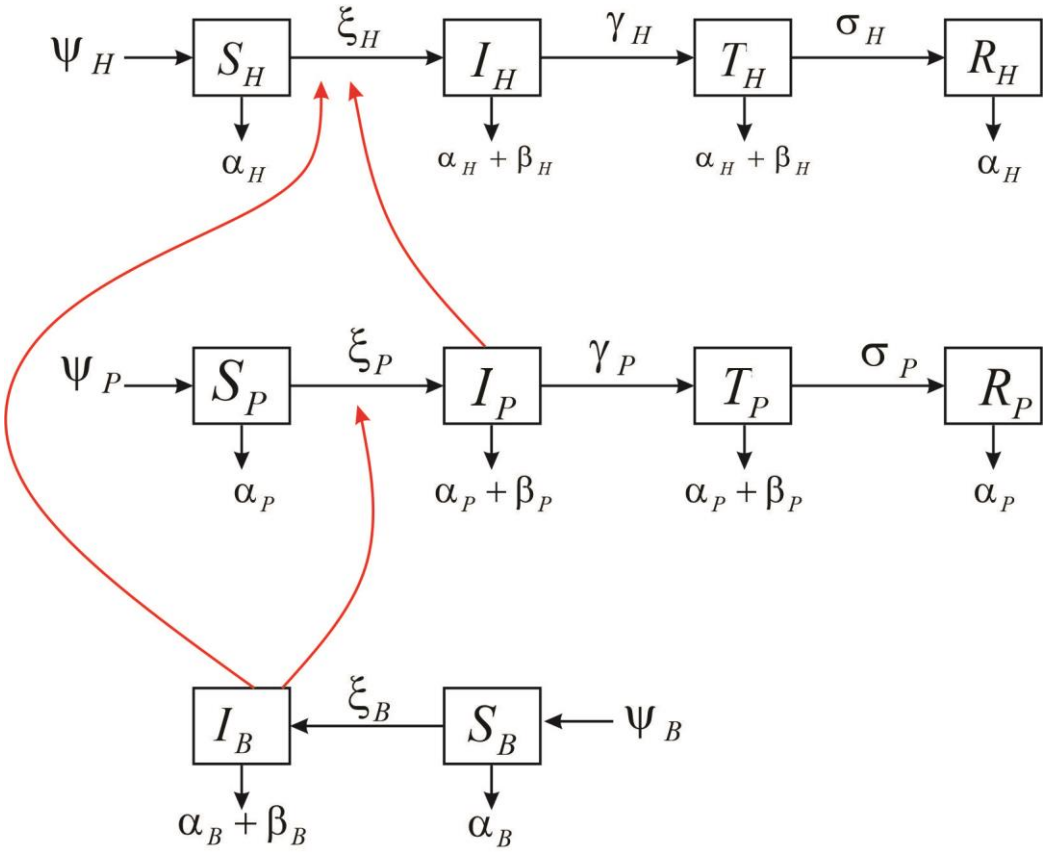

Figure 2: *Schematic diagram of Nipah Virus Transmission*

The Nipah Virus Model's Equations

$$\left.\begin{aligned}
\frac{dS_H}{dt} &= \psi_H - (\xi_H + \alpha_H)S_H \\
\frac{dI_H}{dt} &= \xi_H S_H - (\gamma_H + \alpha_H + \beta_H)I_H \\
\frac{dT_H}{dt} &= \gamma_H I_H - (\sigma_H + \alpha_H + \beta_H)T_H \\
\frac{dR_H}{dt} &= \sigma_H T_H - \alpha_H R_H \\
\frac{dS_P}{dt} &= \psi_P - (\xi_P + \alpha_P)S_P \\
\frac{dI_P}{dt} &= \xi_P S_p - (\gamma_P + \alpha_P + \beta_P)I_P \\
\frac{dT_P}{dt} &= \gamma_P I_P - (\sigma_P + \alpha_P + \beta_P)T_P \\
\frac{dR_P}{dt} &= \sigma_P T_P - \alpha_P R_P \\
\frac{dS_B}{dt} &= \psi_B - (\xi_B + \alpha_B)S_B \\
\frac{dI_B}{dt} &= \xi_B S_B - (\alpha_B + \beta_B)I_B
\end{aligned}\right\} \quad (2)$$

Mathematical Analysis of the Nipah virus Model

Positivity and boundedness of the solution

The differential equation for the human class,

$N_H = S_H + I_H + T_H + R_H$

is given by:

$$\frac{dN_H}{dt} = \frac{dS_H}{dt} + \frac{dI_H}{dt} + \frac{dT_H}{dt} + \frac{dR_H}{dt}$$

Upon substituting the model system of equations for the human class from equation (2) into the preceding equation and correctly performing the elimination process, the result will be

$$\frac{dN_H}{dt} = \psi_H - \alpha_H N_H - \beta_H (I_H + T_H) \quad (4)$$

For the pig population, the equivalent differential equation is written as:

$$\frac{dN_P}{dt} = \psi_P - \alpha_P N_P - \beta_P (I_P + T_P) \quad (5)$$

Furthermore, for the bird society, the equivalent differential equation is written as:

$$\frac{dN_B}{dt} = \psi_B - \alpha_B N_B - \beta_B I_B \tag{6}$$

Theorem 1: Let $(S_H, I_H, T_H, R_H, S_P, I_P, T_P, R_P, S_B, I_B)$ be the solution of the monkey pox model equation (2) with the initial conditions in a biologically feasible region $\Gamma = \Gamma_H \times \Gamma_P \times \Gamma_B$ with:

$$\Gamma_H = \left(S_H, I_H, T_H, R_H\right) \in R_+^4 : N_H \le \frac{\psi_H}{\alpha_H} \tag{7}$$

Likewise

$$\Gamma_P = \left(S_P, I_P, T_P, R_P\right) \in R_+^4 : N_P \le \frac{\psi_P}{\alpha_P} \tag{8}$$

And

$$\Gamma_B = \left(S_B, I_B\right) \in R_+^2 : N_B \le \frac{\psi_B}{\alpha_B} \tag{9}$$

We then have that Γ is non-negative invariant.
Using the integrating factor method to solve equation (4) gives,

$$\frac{dN_H}{dt} = \psi_H - \alpha_H N_H$$

Where $\beta_H = 0$ at DFE

$$\therefore \lim_{t\to\infty} N_H \le \frac{\psi_H}{\alpha_H} \tag{10}$$

Similarly, by utilizing the integrating factor approach to solve equation (5), we obtain:

$$\frac{dN_P}{dt} = \psi_P - \alpha_P N_P$$

Where $\beta_P = 0$ at DFE

$$\therefore \lim_{t\to\infty} N_P \le \frac{\psi_P}{\alpha_P} \tag{11}$$

Lastly, by utilizing the integrating factor approach to solve equation (6), we obtain:

$$\frac{dN_B}{dt} = \psi_B - \alpha_B N_B$$

Where $\beta_B = 0$ at DFE

$$\therefore \lim_{t\to\infty} N_B \le \frac{\psi_B}{\alpha_B} \tag{12}$$

Here, we have confirmed that the model is well-posed mathematically and epidemiologically, and the solutions for the different compartments are non-negative. Equations (10), (11) and (12) lead us to the conclusion that the set is positively invariant for time (t).

Existence of the Nipah Virus equilibrium state

The existence of the Nipah Virus equilibrium state refers to a specific condition in the mathematical model where the Nipah virus is not present or has been eradicated.

Thus, $S_H^0 \neq 0$, $S_P^0 \neq 0$ and $S_B^0 \neq 0$

For $S_H^0 \neq 0, I_H^0 = 0, T_H^0 = 0, R_H^0 = 0$, for $S_P^0 \neq 0, I_P^0 = 0, T_P^0 = 0, R_P^0 = 0$

And for $S_B^0 \neq 0, I_B^0 = 0$

Then, the equations (4), (5) and (6) become

$$\psi_H - \alpha_H S_H^o = 0$$
$$\psi_P - \alpha_P S_P^o = 0$$
$$\psi_B - \alpha_B S_B^o = 0$$

These give

$$S_H^o = \frac{\psi_H}{\alpha_H}, S_P^o = \frac{\psi_P}{\alpha_P} \text{ and } S_B^o = \frac{\psi_B}{\alpha_B} \tag{13}$$

We now have the DFE point to be

$$E^0 = \left(S_H^0, I_H^0, T_H^0, R_H^0, S_P^0, I_P^0, T_P^0, R_P^0, S_B^0, I_B^0\right) = \left(\frac{\psi_H}{\alpha_H}, 0,0,0, \frac{\psi_P}{\alpha_P}, 0,0,0, \frac{\psi_B}{\alpha_B}, 0\right)$$

Basic reproduction number

The basic reproductive ration of Nipah Virus model's system equation (2) is obtained via the method of next generation matrix formulated by Diekmann and Heesterbeek. Using $R_n = \rho(FV^{-1})$ the new infection terms, T_H and transition terms, U_H of system (2) are respectively given as;

$$T_H = \begin{bmatrix} \xi_H S_H \\ 0 \\ \xi_P S_P \\ 0 \\ \xi_B S_B \end{bmatrix} = \begin{bmatrix} t_1 \\ t_2 \\ t_3 \\ t_4 \\ t_5 \end{bmatrix} and, U_H = \begin{bmatrix} (\gamma_H + \alpha_H + \beta_H) I_H \\ -\gamma_H I_H + (\sigma_H + \alpha_H + \beta_H) T_H \\ (\gamma_P + \alpha_P + \beta_P) I_P \\ -\gamma_P I_P + (\sigma_P + \alpha_P + \beta_P) T_P \\ (\alpha_B + \beta_B) I_B \end{bmatrix} = \begin{bmatrix} u_1 \\ u_2 \\ u_3 \\ u_4 \\ u_5 \end{bmatrix} \tag{14}$$

Where $\xi_B = \lambda_B\left(\frac{\phi_B I_B}{N_B}\right); \xi_P = \lambda_P\left(\frac{\phi_B I_B + \phi_P I_P}{N_P}\right); \xi_H = \lambda_H\left(\frac{\phi_B I_B + \phi_P I_P + \phi_H I_H}{N_H}\right)$

$$\text{Let, } F = \begin{bmatrix} \frac{\partial t_1}{\partial I_H} & \frac{\partial t_1}{\partial T_H} & \frac{\partial t_1}{\partial I_P} & \frac{\partial t_1}{\partial T_P} & \frac{\partial t_1}{\partial I_B} \\ \frac{\partial t_2}{\partial I_H} & \frac{\partial t_2}{\partial T_H} & \frac{\partial t_2}{\partial I_P} & \frac{\partial t_2}{\partial T_P} & \frac{\partial t_2}{\partial I_B} \\ \frac{\partial t_3}{\partial I_H} & \frac{\partial t_3}{\partial T_H} & \frac{\partial t_3}{\partial I_P} & \frac{\partial t_3}{\partial T_P} & \frac{\partial t_3}{\partial I_B} \\ \frac{\partial t_4}{\partial I_H} & \frac{\partial t_4}{\partial T_H} & \frac{\partial t_4}{\partial I_P} & \frac{\partial t_4}{\partial T_P} & \frac{\partial t_4}{\partial I_B} \\ \frac{\partial t_5}{\partial I_H} & \frac{\partial t_5}{\partial T_H} & \frac{\partial t_5}{\partial I_P} & \frac{\partial t_5}{\partial T_P} & \frac{\partial t_5}{\partial I_B} \end{bmatrix} \text{ and } V = \begin{bmatrix} \frac{\partial u_1}{\partial I_H} & \frac{\partial u_1}{\partial T_H} & \frac{\partial u_1}{\partial I_P} & \frac{\partial u_1}{\partial T_P} & \frac{\partial u_1}{\partial I_B} \\ \frac{\partial u_2}{\partial I_H} & \frac{\partial u_2}{\partial T_H} & \frac{\partial u_2}{\partial I_P} & \frac{\partial u_2}{\partial T_P} & \frac{\partial u_2}{\partial I_B} \\ \frac{\partial u_3}{\partial I_H} & \frac{\partial u_3}{\partial T_H} & \frac{\partial u_3}{\partial I_P} & \frac{\partial u_3}{\partial T_P} & \frac{\partial u_3}{\partial I_B} \\ \frac{\partial u_4}{\partial I_H} & \frac{\partial u_4}{\partial T_H} & \frac{\partial u_4}{\partial I_P} & \frac{\partial u_4}{\partial T_P} & \frac{\partial u_4}{\partial I_B} \\ \frac{\partial u_5}{\partial I_H} & \frac{\partial u_5}{\partial T_H} & \frac{\partial u_5}{\partial I_P} & \frac{\partial u_5}{\partial T_P} & \frac{\partial u_5}{\partial I_B} \end{bmatrix} \tag{15}$$

So we have

$$F = \begin{bmatrix} \lambda_H\phi_H & 0 & \lambda_P\phi_P & 0 & \lambda_B\phi_B \\ 0 & 0 & 0 & 0 & 0 \\ 0 & 0 & \lambda_P\phi_P & 0 & \lambda_B\phi_B \\ 0 & 0 & 0 & 0 & 0 \\ 0 & 0 & 0 & 0 & \lambda_B\phi_B \end{bmatrix} \tag{16}$$

and

$$V = \begin{bmatrix} \gamma_H+\alpha_H+\beta_H & 0 & 0 & 0 & 0 \\ -\gamma_H & \sigma_H+\alpha_H+\beta_H & 0 & 0 & 0 \\ 0 & 0 & \gamma_P+\alpha_P+\beta_P & 0 & 0 \\ 0 & 0 & 0 & \sigma_P+\alpha_P+\beta_P & 0 \\ 0 & 0 & 0 & 0 & \alpha_B+\beta_B \end{bmatrix} \tag{17}$$

$$FV^{-1} = \begin{bmatrix} \frac{\lambda_H\phi_H}{\gamma_H+\alpha_H+\beta_H} & 0 & \frac{\lambda_P\phi_P}{\gamma_P+\alpha_P+\beta_P} & 0 & \frac{\lambda_B\phi_B}{\alpha_B+\beta_B} \\ 0 & 0 & 0 & 0 & 0 \\ 0 & 0 & \frac{\lambda_P\phi_P}{\gamma_P+\alpha_P+\beta_P} & 0 & \frac{\lambda_B\phi_B}{\alpha_B+\beta_B} \\ 0 & 0 & 0 & 0 & 0 \\ 0 & 0 & 0 & 0 & \frac{\lambda_B\phi_B}{\alpha_B+\beta_B} \end{bmatrix} \tag{18}$$

Therefore, we have the basic reproduction number, $R_n = \rho(FV^{-1})$, for the human class, pig population and bird society to be

$$R_H = \frac{\lambda_H\phi_H}{\gamma_H+\alpha_H+\beta_H};\ R_P = \frac{\lambda_P\phi_P}{\gamma_P+\alpha_P+\beta_P} \text{ and } R_B = \frac{\lambda_B\phi_B}{\alpha_B+\beta_B} \tag{19}$$

respectively.

Local Stability of Disease-Free Equilibrium

To determine the local stability of the Nipah virus DFE, we calculate the eigenvalues of the Jacobian matrix estimated at the DFE. The Jacobian matrix describes the linearization of the model equations of the Nipah virus around the DFE, and its eigenvalues provide information about the stability of the Nipah virus DFE.

Theorem 2:
If every Jacobian eigenvalue of the system has a negative real value, the disease-free equilibrium of the model equation (2) is locally asymptotically stable (LAS).

Proof
We evaluate the eigenvalues of the Jacobian matrix of the model's equation in (2) at DFE point

$\left(\frac{\psi_H}{\alpha_H},0,0,0,\frac{\psi_P}{\alpha_P},0,0,0,\frac{\psi_B}{\alpha_B},0\right)$ in order for us to prove the above-mentioned theorem. The Jacobian matrix

$J(S_H, I_H, T_H, R_H, S_P, I_P, T_P, R_P, S_B, I_B)$ of the model is given as:

$$J=\begin{bmatrix} -\alpha_H & -\lambda_H\phi_H & 0 & 0 & 0 & -\lambda_P\phi_P & 0 & 0 & 0 & -\lambda_B\phi_B \\ 0 & -b & 0 & 0 & 0 & \lambda_P\phi_P & 0 & 0 & 0 & \lambda_B\phi_B \\ 0 & \gamma_H & -c & 0 & 0 & 0 & 0 & 0 & 0 & 0 \\ 0 & 0 & \sigma_H & -\alpha_H & 0 & 0 & 0 & 0 & 0 & 0 \\ 0 & 0 & 0 & 0 & -\alpha_P & -\lambda_P\phi_P & 0 & 0 & 0 & -\lambda_B\phi_B \\ 0 & 0 & 0 & 0 & 0 & -d & 0 & 0 & 0 & \lambda_B\phi_B \\ 0 & 0 & 0 & 0 & 0 & \gamma_P & -e & 0 & 0 & 0 \\ 0 & 0 & 0 & 0 & 0 & 0 & \sigma_P & -\alpha_P & 0 & 0 \\ 0 & 0 & 0 & 0 & 0 & 0 & 0 & 0 & -\alpha_B & -\lambda_B\phi_B \\ 0 & 0 & 0 & 0 & 0 & 0 & 0 & 0 & 0 & -f \end{bmatrix} \quad (20)$$

where $b=-\lambda_H\phi_H+\gamma_H+\alpha_H+\beta_H$; $c=\sigma_H+\alpha_H+\beta_H$; $d=-\lambda_P\phi_P+\gamma_P+\alpha_P+\beta_{PH}$; $e=\sigma_P+\alpha_P+\beta_P$; and $f=-\lambda_B\phi_B+\alpha_B+\beta_B$

Now, for the eigenvalue computation, we have the following steps:

$$|J-\lambda I|=\begin{vmatrix} -\alpha_H-\lambda & -\lambda_H\phi_H & 0 & 0 & 0 & -\lambda_P\phi_P & 0 & 0 & 0 & -\lambda_B\phi_B \\ 0 & -b-\lambda & 0 & 0 & 0 & \lambda_P\phi_P & 0 & 0 & 0 & \lambda_B\phi_B \\ 0 & \gamma_H & -c-\lambda & 0 & 0 & 0 & 0 & 0 & 0 & 0 \\ 0 & 0 & \sigma_H & -\alpha_H-\lambda & 0 & 0 & 0 & 0 & 0 & 0 \\ 0 & 0 & 0 & 0 & -\alpha_P-\lambda & -\lambda_P\phi_P & 0 & 0 & 0 & -\lambda_B\phi_B \\ 0 & 0 & 0 & 0 & 0 & -d-\lambda & 0 & 0 & 0 & \lambda_B\phi_B \\ 0 & 0 & 0 & 0 & 0 & \gamma_P & -e-\lambda & 0 & 0 & 0 \\ 0 & 0 & 0 & 0 & 0 & 0 & \sigma_P & -\alpha_P-\lambda & 0 & 0 \\ 0 & 0 & 0 & 0 & 0 & 0 & 0 & 0 & -\alpha_B-\lambda & -\lambda_B\phi_B \\ 0 & 0 & 0 & 0 & 0 & 0 & 0 & 0 & 0 & -f-\lambda \end{vmatrix} \quad (21)$$

From above matrix (21), $\lambda_1=-\alpha_H$ as $-\alpha_H-\lambda$ happens to be the only non-zero element in the first column. We delete the first row and first column to get a new matrix J^1 as;

$$J^1 = \begin{vmatrix} -b-\lambda & 0 & 0 & 0 & \lambda_P\phi_P & 0 & 0 & 0 & \lambda_B\phi_B \\ \gamma_H & -c-\lambda & 0 & 0 & 0 & 0 & 0 & 0 & 0 \\ 0 & \sigma_H & -\alpha_H-\lambda & 0 & 0 & 0 & 0 & 0 & 0 \\ 0 & 0 & 0 & -\alpha_P-\lambda & -\lambda_P\phi_P & 0 & 0 & 0 & -\lambda_B\phi_B \\ 0 & 0 & 0 & 0 & -d-\lambda & 0 & 0 & 0 & \lambda_B\phi_B \\ 0 & 0 & 0 & 0 & \gamma_P & -e-\lambda & 0 & 0 & 0 \\ 0 & 0 & 0 & 0 & 0 & \sigma_P & -\alpha_P-\lambda & 0 & 0 \\ 0 & 0 & 0 & 0 & 0 & 0 & 0 & -\alpha_B-\lambda & -\lambda_B\phi_B \\ 0 & 0 & 0 & 0 & 0 & 0 & 0 & 0 & -f-\lambda \end{vmatrix} \quad (22)$$

Similarly in column 3 of above matrix (22), $-\alpha_H - \lambda$ is the only entry and so $\lambda_2 = -\alpha_H$. We then have a new matrix J^2 as

$$J^2 = \begin{vmatrix} -b-\lambda & 0 & 0 & \lambda_P\phi_P & 0 & 0 & 0 & \lambda_B\phi_B \\ \gamma_H & -c-\lambda & 0 & 0 & 0 & 0 & 0 & 0 \\ 0 & 0 & -\alpha_P-\lambda & -\lambda_P\phi_P & 0 & 0 & 0 & -\lambda_B\phi_B \\ 0 & 0 & 0 & -d-\lambda & 0 & 0 & 0 & \lambda_B\phi_B \\ 0 & 0 & 0 & \gamma_P & -e-\lambda & 0 & 0 & 0 \\ 0 & 0 & 0 & 0 & \sigma_P & -\alpha_P-\lambda & 0 & 0 \\ 0 & 0 & 0 & 0 & 0 & 0 & -\alpha_B-\lambda & -\lambda_B\phi_B \\ 0 & 0 & 0 & 0 & 0 & 0 & 0 & -f-\lambda \end{vmatrix} \quad (23)$$

Similarly in column 2 in the matrix above, we have $-c-\lambda$ as the only entry. Hence $\lambda_3 = -c$,
Following the above procedure, writing out the emerging Jacobian matrix and deleting elements where necessary we obtain the eigenvalues of the 10 – dimensional system as:

$$\lambda_1 = -\alpha_H, \lambda_2 = -\alpha_H, \lambda_3 = -c, \lambda_4 = -b, \lambda_5 = -d, \lambda_6 = -e, \lambda_7 = -\alpha_p, \lambda_8 = -\alpha_p, \lambda_9 = -\alpha_B, \lambda_{10} = -f \quad (24$$

learly, the eigenvalues are real, negative and not complex which shows that the Nipah virus DFE is locally asymptotically stable.

Theorem 3
When $R_H < 1$, $R_P < 1$ and $R_B < 1$, then the disease-free equilibrium is locally asymptotically stable.

Proof
We obtained in the eigenvalues that $\lambda_4 = -(-\lambda_H\phi_H + \gamma_H + \alpha_H + \beta_H)$, $\lambda_5 = -\left(-\phi_P + \gamma_P + \alpha_P + \beta_P\right)$ and $\lambda_{10} = -\left(-\lambda_B\phi_B + \alpha_B + \beta_B\right)$

Lemma 1
When $R_H < 1$, $R_P < 1$ and $R_B < 1$ respectively, the disease-free equilibrium for the human class, pig population and bird society are asymptotically stable.

The eigenvalues above can be factorized as;

$$\begin{aligned}
\lambda_4 &= \lambda_H \phi_H \left(1 - \frac{\lambda_H \phi_H}{\gamma_H + \alpha_H + \beta_H}\right) \\
\lambda_5 &= \lambda_P \phi_P \left(1 - \frac{\lambda_P \phi_P}{\gamma_P + \alpha_P + \beta_P}\right) \\
\lambda_{10} &= \lambda_B \phi_B \left(1 - \frac{\lambda_B \phi_B}{\alpha_B + \beta_B}\right)
\end{aligned} \tag{25}$$

From (23) we can write that;

$$\begin{aligned}
\lambda_4 &= \lambda_H \phi_H \left(1 - \frac{\lambda_H \phi_H}{\gamma_H + \alpha_H + \beta_H}\right) \le \lambda_H \phi_H (1 - R_H) \\
\lambda_5 &= \lambda_P \phi_P \left(1 - \frac{\lambda_P \phi_P}{\gamma_P + \alpha_P + \beta_P}\right) \le \lambda_P \phi_P (1 - R_P) \\
\lambda_{10} &= \lambda_B \phi_B \left(1 - \frac{\lambda_B \phi_B}{\alpha_B + \beta_B}\right) \le \lambda_B \phi_B (1 - R_B)
\end{aligned} \tag{26}$$

The inequalities (25) and (26) remain true and negative (stable) if and only if $R_H < 1$, $R_P < 1$ and $R_B < 1$. This proves lemma 1.
Moving forward with the proof of Theorem 3, we establish that $R_H < 1$, $R_P < 1$ and $R_B < 1$ holds.

Global Stability of Disease-Free Equilibrium (DFE)

Theorem 4
The non-negative equilibrium point of the model (2) is globally asymptotically stable, if $G^0 > 1$.

Proof
To establish the global stability of this equilibrium E^0, we construct the following Lyapunov function following the method used in [46].

$$\begin{aligned}
&G(S_H, I_H, T_H, R_H, S_P, I_P, T_P, R_P, S_B, I_B) = \\
&\left(S_H - S_H^0 - S_H^0 \log \frac{S_H^0}{S_H}\right) + \left(I_H - I_H^0 - I_H^0 \log \frac{I_H^0}{I_H}\right) \\
&+ \left(T_H - T_H^0 - T_H^0 \log \frac{T_H^0}{T_H}\right) + \left(R_H - R_H^0 - R_H^0 \log \frac{R_H^0}{R_H}\right) \\
&+ \left(S_P - S_P^0 - S_P^0 \log \frac{S_P^0}{S_P}\right) + \left(I_P - I_P^0 - I_P^0 \log \frac{I_P^0}{I_P}\right) \\
&+ \left(T_P - T_P^0 - T_p^0 \log \frac{T_P^0}{T_P}\right) + \left(R_P - R_P^0 - R_P^0 \log \frac{R_P^0}{R_P}\right) \\
&+ \left(S_B - S_B^0 - S_B^0 \log \frac{S_B^0}{S_B}\right) + \left(I_B - I_B^0 - I_B^0 \log \frac{I_B^0}{I_B}\right)
\end{aligned} \tag{27}$$

The derivative of G along the solution path of (2) by direct calculation gives

$$\begin{aligned}\frac{dG}{dt} &= \left(\frac{S_H - S_H^0}{S_H}\right)\frac{dS_H}{dt} + \left(\frac{I_H - I_H^0}{I_H}\right)\frac{dI_H}{dt} + \left(\frac{T_H - T_H^0}{T_H}\right)\frac{dT_H}{dt} \\ &+ \left(\frac{R_H - R_H^0}{R_H}\right)\frac{dR_H}{dt} + \left(\frac{S_P - S_P^0}{S_P}\right)\frac{dS_P}{dt} + \left(\frac{I_P - I_P^0}{I_P}\right)\frac{dI_P}{dt} + \left(\frac{T_P - T_P^0}{T_P}\right)\frac{dT_P}{dt} \\ &+ \left(\frac{R_P - R_P^0}{R_P}\right)\frac{dR_P}{dt} + \left(\frac{S_B - S_B^0}{S_B}\right)\frac{dS_B}{dt} + \left(\frac{I_B - I_B^0}{I_B}\right)\frac{dI_B}{dt}\end{aligned} \tag{28}$$

We expand the above equation and collect the positive and negative terms separately, where the positive term is P and the negative term is N, then

$$\frac{dG}{dt} = P - N$$

$$\begin{aligned}P &= \left(1 - \frac{S_H^0}{S_H}\right)\psi_H + \left(1 - \frac{I_H^0}{I_H}\right)\xi_H S_H + \left(1 - \frac{T_H^0}{T_H}\right)\gamma_H I_H \\ &+ \left(1 - \frac{R_H^0}{R_H}\right)\sigma_H T_H + \left(1 - \frac{S_P^0}{S_P}\right)\psi_P + \left(1 - \frac{I_P^0}{I_P}\right)\xi_P S_P + \left(1 - \frac{T_P^0}{T_P}\right)\gamma_P I_P \\ &+ \left(1 - \frac{R_P^0}{R_P}\right)\sigma_P T_P + \left(1 - \frac{S_B^0}{S_B}\right)\psi_B + \left(1 - \frac{I_B^0}{I_B}\right)\xi_B S_B\end{aligned} \tag{29}$$

Similarly,

$$\begin{aligned}N &= \frac{\left(S_H - S_H^0\right)^2}{S_H}\left(\xi_H + \alpha_H\right) + \frac{\left(I_H - I_H^0\right)^2}{I_H}\left(\gamma_H + \alpha_H + \beta_H\right) + \frac{\left(T_H - T_H^0\right)^2}{T_H}\left(\sigma_H + \alpha_H + \beta_H\right) \\ &+ \frac{\left(R_H - R_H^0\right)^2}{R_H}\alpha_H + \frac{\left(S_P - S_P^0\right)^2}{S_P}\left(\xi_P + \alpha_P\right) + \frac{\left(I_P - I_P^0\right)^2}{I_P}\left(\gamma_P + \alpha_p + \beta_P\right) + \frac{\left(T_P - T_P^0\right)^2}{T_P}\left(\sigma_P + \alpha_P + \beta_P\right) \\ &+ \frac{\left(R_P - R_P^0\right)^2}{R_P}\alpha_P + \frac{\left(S_B - S_B^0\right)^2}{S_B}\left(\xi_B + \alpha_B\right) + \frac{\left(I_B - I_B^0\right)^2}{I_B}\left(\alpha_B + \beta_B\right)\end{aligned} \tag{30}$$

If $P < N$, then $\frac{dG}{dt}$ will be negative definite along the solution path of the system. And thus, implies that, only at Nipah disease free equilibrium (E0) would $\frac{dG}{dt} \le 0$. This indicates that the system is globally stable at the Nipah virus disease free equilibrium.

Existence of the endemic equilibrium points

The endemic equilibrium points are defined as $\left(S_H^*(t), 0, 0, 0, S_P^*(t), 0, 0, 0, S_B^*(t), 0\right)$ satisfying $\left(S_H' = I_H' = T_H' = R_H' = S_P' = I_P' = T_P' = R_P' = S_B' = I_B = 0\right)$, by equating equation (2) to zero, we have

$$\left.\begin{aligned}
&\psi_H-(\xi_H+\alpha_H)S_H^*=0\\
&\xi_H S_H^*-(\gamma_H+\alpha_H+\beta_H)I_H^*=0\\
&\gamma_H I_H^*-(\sigma_H+\alpha_H+\beta_H)T_H^*=0\\
&\sigma_H T_H^*-\alpha_H R_H^*=0\\
&\psi_P-(\xi_P+\alpha_P)S_P^*=0\\
&\xi_P S_P^*-(\gamma_P+\alpha_P+\beta_P)I_P^*=0\\
&\gamma_P I_P^*-(\sigma_P+\alpha_P+\beta_P)T_P^*=0\\
&\sigma_P T_P^*-\alpha_P R_P^*=0\\
&\psi_B-(\xi_B+\alpha_B)S_B^*=0\\
&\xi_B S_B^*-(\alpha_B+\beta_B)I_B^*=0
\end{aligned}\right\} \tag{31}$$

where;

$$\xi_B=\lambda_B\left(\frac{\phi_B I_B}{N_B}\right);\xi_P=\lambda_P\left(\frac{\phi_B I_B+\phi_P I_P}{N_P}\right);\xi_H=\lambda_H\left(\frac{\phi_B I_B+\phi_P I_P+\phi_H I_H}{N_H}\right) \tag{32}$$

Simplify the equation accordingly we have,

$$\begin{aligned}
&S_H^*=\frac{\psi_H}{(\xi_H+\alpha_H)};\ I_H^*=\frac{\xi_H\psi_H}{(\gamma_H+\alpha_H+\beta_H)(\xi_H+\alpha_H)};\\
&T_H^*=\frac{\xi_H\psi_H\gamma_H}{(\sigma_H+\alpha_H+\beta_H)(\gamma_H+\alpha_H+\beta_H)(\xi_H+\alpha_H)};\\
&R_H^*=\frac{\xi_H\psi_H\gamma_H\sigma_H}{\alpha_H(\sigma_H+\alpha_H+\beta_H)(\gamma_H+\alpha_H+\beta_H)(\xi_H+\alpha_H)}\\
&S_P^*=\frac{\psi_P}{(\xi_P+\alpha_P)};\ I_P^*=\frac{\xi_P\psi_P}{(\gamma_P+\alpha_P+\beta_P)(\xi_P+\alpha_P)};\\
&T_P^*=\frac{\xi_P\psi_P\gamma_P}{(\sigma_P+\alpha_P+\beta_P)(\gamma_P+\alpha_P+\beta_P)(\xi_P+\alpha_P)};\\
&R_P^*=\frac{\xi_P\psi_P\gamma_P\sigma_P}{\alpha_P(\sigma_P+\alpha_P+\beta_P)(\gamma_P+\alpha_P+\beta_P)(\xi_P+\alpha_P)};\\
&S_B^*=\frac{\psi_B}{(\xi_B+\alpha_B)};\ I_B^*=\frac{\xi_H\psi_B}{(\alpha_B+\beta_B)(\xi_B+\alpha_B)};
\end{aligned} \tag{33}$$

Using the conventional methods, at E^0, the existence of the endemic equilibrium points are established.

Sensitivity analysis of the reservoirs-human model

In sensitivity analysis, different parameters are varied within their respective plausible ranges, and the model's response is observed. This variation can be done individually (one-at-a-time sensitivity analysis) or collectively (global sensitivity analysis) for multiple parameters simultaneously.

As a result, we analyze the reproduction number of the model which looks for variation and the impact of a parameter's value on reproduction number whether it is raised or lowered.

Definition

The definition of the Normalized Forward-Sensitivity Index of a variable U, which is differentially dependent on a parameter V, is as follows:

$$X_V^U = \frac{\partial U}{\partial V} \cdot \frac{V}{U} \tag{34}$$

Regarding the model parameters, we will now calculate the sensitivity indices for the fundamental reproduction number R_H, R_P, and R_B.

$$R_H = \frac{\lambda_H \phi_H}{\gamma_H + \alpha_H + \beta_H};\ R_P = \frac{\lambda_P \phi_P}{\gamma_P + \alpha_P + \beta_P};\ \text{and}\ R_B = \frac{\lambda_B \phi_B}{\alpha_B + \beta_B}$$

Sensitivity index for ϕ_H

The normalized forward sensitivity index of ϕ_H is given by:

$$X_{\phi_H}^{R_H} = \frac{\partial R_H}{\partial \phi_H} \cdot \frac{\phi_H}{R_H} \tag{35}$$

By Computing and evaluating the derivatives in (35), we have;

$$\frac{\partial R_H}{\partial \phi_H} = \frac{1}{\phi_H} R_H \tag{36}$$

Then,

$$X_{\phi_H}^{R_H} = \frac{\partial R_H}{\partial \phi_H} \cdot \frac{\phi_H}{R_H} = \frac{1}{\phi_H} R_n \cdot \frac{\phi_H}{R_n}$$

$$\therefore X_{\phi_H}^{R_H} = +1 \tag{37}$$

As a result, we get the sensitivity index ϕ_H.

The sensitivity indices of all other parameters in the fundamental reproduction number are also obtained using the same procedure, which is consistently applied.

Table 2: Sensitivity indices pertaining to additional parameters within the context of the basic reproductive ration.

Parameters	Values	Source	Index sign	Sensitivity Index value
ϕ_H	0.0015	Scot et. al [46]	+	1
ϕ_P	0.02	Scot et. al [46]	+	1
ϕ_B	0.2	Scot et. al [46]	+	1
γ_H	0.0001	Zewdie and Gakhar [47]	-	-0.04668316138
γ_P	0.0002	Zewdie and Gakhar [47]	-	-0.001240694789
α_H	0.0000421	Zewdie and Gakhar [47]	-	-0.01965361094
α_P	0.16	Tyagi et. al [48]	-	-0.9925558313
α_B	0.45	Scot et. al [46]	-	-0.375000000
β_B	0.75	Zewdie and Gakhar [47]	-	-0.6250000000
β_P	0.001	Scot et. al [46]	-	-0.006203473945
β_H	0.002	Tyagi et. al [48]	-	-0.9336632276
λ_H	0.0002	Zewdie and Gakhar [47]	+	1
λ_P	0.01	Zewdie and Gakhar [47]	+	1
λ_B	0.1	Zewdie and Gakhar [47]	+	1

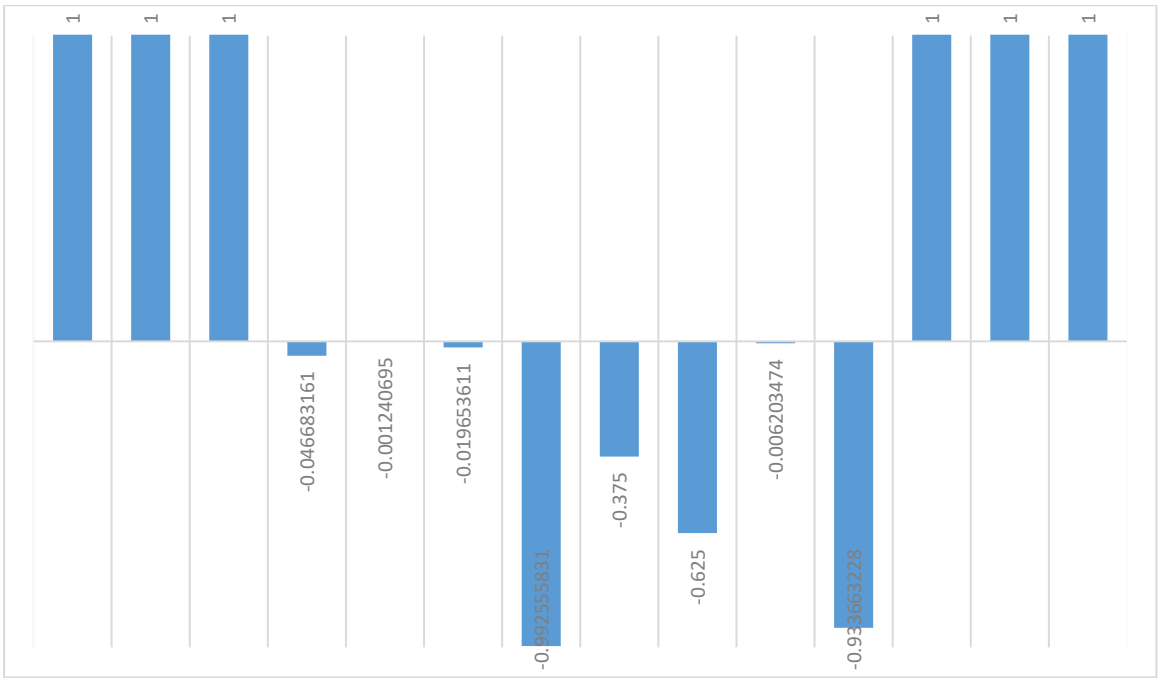

Interpretation of Sensitivity Indices

A negative sensitivity index indicates an inverse relationship between the parameter and the reproduction number. In contrast, a positive sensitivity index implies that an increase in the parameter value leads to a higher value of the reproduction number. This analysis helps identify which parameters strongly influence the results of our analysis.

Optimal Control Strategies for Nipah virus

Here are some key components of optimal control for Nipah virus: we lower the transmission rate by $(1-C_1)$, where C_1 connotes personal prevention (practice handwashing, avoid contact with sick birds or pigs, avoid eating or drinking products that could be contaminated by bats and avoid contact with the blood or body fluids of any person known to be infected; C_2 connotes the effort of treatment on the infected human class. C_3 connotes biosecurity measures and public health intervention C_4 connotes the effort of treatment on the pig population. Based on these assumptions, the following set of new equations is derived:

$$\left.\begin{aligned}
\frac{dS_H}{dt} &= \psi_H - \left((1-C_1)\xi_H + \alpha_H\right)S_H \\
\frac{dI_H}{dt} &= (1-C_1)\xi_H S_H - (C_2 + \alpha_H + \beta_H)I_H \\
\frac{dT_H}{dt} &= C_2 I_H - (\sigma_H + \alpha_H + \beta_H)T_H \\
\frac{dR_H}{dt} &= \sigma_H T_H - \alpha_H R_H \\
\frac{dS_P}{dt} &= \psi_P - \left((1-C_3)\xi_P + \alpha_P\right)S_P \\
\frac{dI_P}{dt} &= (1-C_3)\xi_P S_p - (C_4 + \alpha_P + \beta_P)I_P \\
\frac{dT_P}{dt} &= C_4 I_P - (\sigma_P + \alpha_P + \beta_P)T_P \\
\frac{dR_P}{dt} &= \sigma_P T_P - \alpha_P R_P \\
\frac{dS_B}{dt} &= \psi_B - (\xi_B + \alpha_B)S_B \\
\frac{dI_B}{dt} &= \xi_B S_B - (\alpha_B + \beta_B)I_B
\end{aligned}\right\} \quad (38)$$

$$\xi_B = \lambda_B\left(\frac{\phi_B I_B}{N_B}\right); \xi_P = \lambda_P\left(\frac{\phi_B I_B + \phi_P I_P}{N_P}\right); \xi_H = \lambda_H\left(\frac{\phi_B I_B + \phi_P I_P + \phi_H I_H}{N_H}\right)$$

Analysis of the Model Incorporating Preventive Measures

Within this segment, we constructed a model centered on an objective functional framework, showcasing the potential for manipulation through the utilization of Pontryagin's Maximum Principle. By focusing on the optimal configuration outlined in the system of equation (18), we have highlighted the emergence of a significant control concern, which we subsequently elucidated before delving into its comprehensive global optimization. The intricate task of selecting the most efficacious strategies is encapsulated by the objective functional denoted as H. The overarching pre-established aim entails the minimization of the populace in all classes, all within a designated time interval [0, K].

Let $L = \{(C_1, C_2, C_3, C_4) \in L\}$ be Lebesgue measurable on $[0,1]$,

Where $0 \le C_i(t) \le 1 \in [0,1], i = 1,2,3,4$

Then, we have the objective function, O, to be

$$O(C_1, C_2, C_3, C_4) = \int_0^K \left(T_1 T_P + T_2 I_P + T_3 T_H + T_4 I_H + \frac{1}{2}\left(U_1 C_1^2 + U_2 C_2^2 + U_3 C_3^2 + U_4 C_4^2\right)\right) dt \tag{39}$$

constraint to (38)

$$\left.\begin{aligned}
\frac{dS_H}{dt} &= \psi_H - \left((1-C_1)\xi_H + \alpha_H\right)S_H \\
\frac{dI_H}{dt} &= (1-C_1)\xi_H S_H - \left(C_2 + \alpha_H + \beta_H\right)I_H \\
\frac{dT_H}{dt} &= C_2 I_H - \left(\sigma_H + \alpha_H + \beta_H\right)T_H \\
\frac{dR_H}{dt} &= \sigma_H T_H - \alpha_H R_H \\
\frac{dS_P}{dt} &= \psi_P - \left((1-C_3)\xi_P + \alpha_P\right)S_P \\
\frac{dI_P}{dt} &= (1-C_3)\xi_P S_p - \left(C_4 + \alpha_P + \beta_P\right)I_P \\
\frac{dT_P}{dt} &= C_4 I_P - \left(\sigma_P + \alpha_P + \beta_P\right)T_P \\
\frac{dR_P}{dt} &= \sigma_P T_P - \alpha_P R_P \\
\frac{dS_B}{dt} &= \psi_B - \left(\xi_B + \alpha_B\right)S_B \\
\frac{dI_B}{dt} &= \xi_B S_B - \left(\alpha_B + \beta_B\right)I_B
\end{aligned}\right\} \tag{40}$$

The terminal time point is represented by the value K, while the coefficients T_1 to T_4 correspond to the weight constants attributed to the virus within distinct groups. The primary objective of this section centers on the reduction of the operational expenditure as indicated by equation (19). Furthermore, our investigation extends to encompass an analysis of the social cost $U_1 C_1^{\,2}, U_2 C_2^{\,2}, U_3 C_3^{\,2}$, and $U_4 C_4^{\,2}$ associated with the described scenario.

In order to fulfill the aim of addressing the control problem, we endeavor to identify the functions $\left(C_1^*(t), C_2^*(t), C_3^*(t), C_4^*(t)\right)$, such that

$$O\left(C_1^*(t), C_2^*(t), C_3^*(t), C_4^*(t)\right) = \min\{O(C), (C) \in L\} \tag{41}$$

Existence of an Optimal Control Solution

Theorem: From equation (20), Consider $O(C)$, subject to (18) and with t=0 be the initial condition, then given the optimal control to be $C_1^*(t), C_2^*(t), C_3^*(t), C_4^*(t)$ such that

$$O\left(C_1^*(t), C_2^*(t), C_3^*(t), C_4^*(t)\right) = \min\{O(C), (C) \in L\}$$

Proof: Because the integrand of O demonstrates convexity concerning the control measures C the existence of an optimal control solution is ensured.

Next, it is essential to demonstrate the optimal solution. The Lagrangian is expressed as follows:

$$G = T_1 T_P + T_2 I_P + T_3 T_H + T_4 I_H + \frac{1}{2}\left(U_1 C_1^{\,2} + U_2 C_2^{\,2} + U_3 C_3^{\,2} + U_4 C_4^{\,2}\right)t \tag{42}$$

The Hamiltonian function is given as;

$$\begin{aligned} H &= T_1 T_P + T_2 I_P + T_3 T_H + T_4 I_H + \frac{1}{2}\left(U_1 C_1^{\,2} + U_2 C_2^{\,2} + U_3 C_3^{\,2} + U_4 C_4^{\,2}\right)t \\ &+ \Psi_{S_H}\left[S_H^{'}\right] + \Psi_{I_H}\left[I_H^{'}\right] + \Psi_{T_H}\left[T_H^{'}\right] + \Psi_{R_H}\left[R_H^{'}\right] \\ &+ \Psi_{S_P}\left[S_P^{'}\right] + \Psi_{I_P}\left[I_P^{'}\right] + \Psi_{T_P}\left[T_P^{'}\right] + \Psi_{R_P}\left[R_P^{'}\right] \\ &+ \Psi_{S_B}\left[S_B^{'}\right] + \Psi_{I_B}\left[I_B^{'}\right] \end{aligned} \tag{43}$$

and

$$\left.\begin{aligned} \frac{dS_H}{dt} &= \psi_H - ((1-C_1)\xi_H + \alpha_H)S_H \\ \frac{dI_H}{dt} &= (1-C_1)\xi_H S_H - (C_2 + \alpha_H + \beta_H)I_H \\ \frac{dT_H}{dt} &= C_2 I_H - (\sigma_H + \alpha_H + \beta_H)T_H \\ \frac{dR_H}{dt} &= \sigma_H T_H - \alpha_H R_H \\ \frac{dS_P}{dt} &= \psi_P - ((1-C_3)\xi_P + \alpha_P)S_P \\ \frac{dI_P}{dt} &= (1-C_3)\xi_P S_P - (C_4 + \alpha_P + \beta_P)I_P \\ \frac{dT_P}{dt} &= C_4 I_P - (\sigma_P + \alpha_P + \beta_P)T_P \\ \frac{dR_P}{dt} &= \sigma_P T_P - \alpha_P R_P \\ \frac{dS_B}{dt} &= \psi_B - (\xi_B + \alpha_B)S_B \\ \frac{dI_B}{dt} &= \xi_B S_B - (\alpha_B + \beta_B)I_B \end{aligned}\right\} \tag{44}$$

Given $\Psi_i, i \in \{S_H, I_H, T_H, R_H, S_P, I_P, T_P, R_P, S_B, I_B\}$ are distinct and non-overlapping variables.

We are now poised to employ the essential conditions to the Hamiltonian (H) for analysis.

To unveil the adjoint equation and fulfill the transversality condition, we leverage the Hamiltonian H. Through the process of differentiation, we ascertain the values concerning the variables $S_H, I_H, T_H, R_H, S_P, I_P, T_P, R_P, S_B, I_B$ with respect to the Hamiltonian. This leads us to the formulation of the adjoint equation, which is expressed as follows:

$$\frac{d\Psi_{S_H}}{dt} = -\frac{\partial H}{dS_H} = \left[\left((1-C_1)\xi_H\left(1-\frac{S_H}{N_H}\right) + \alpha_H\right)\Psi_{S_H} - \left((1-C_1)\xi_H\left(1-\frac{S_H}{N_H}\right)\right)\Psi_{I_H}\right] \tag{45}$$

$$\frac{d\Psi_{I_H}}{dt} = -\frac{\partial H}{dI_H} = \left[-T^4 + \left((1-C_1)\frac{\lambda_H\phi_H - \xi_H}{N_H}\right)S_H\Psi_{S_H} - \left((1-C_1)\frac{\lambda_H\phi_H - \xi_H}{N_H} - (C_2 + \alpha_H + \beta_H)\right)S_H\Psi_{I_H} - C_2\Psi_{T_H}\right] \tag{46}$$

$$\frac{d\Psi_{T_H}}{dt} = -\frac{\partial H}{dT_H} = \left[-T^3 + \left((1-C_1)\frac{\xi_H}{N_H}\right)S_H\Psi_{S_H} - (1-C_1)\frac{\xi_H}{N_H}S_H\Psi_{I_H} + (\sigma_H + \alpha_H + \beta_H)\Psi_{T_H} - \sigma_H\Psi_{R_H}\right] \tag{47}$$

$$\frac{d\Psi_{R_H}}{dt} = -\frac{\partial H}{dR_H} = \left[\left((1-C_1)\frac{\xi_H}{N_H}\right)S_H\Psi_{S_H} - (1-C_1)\frac{\xi_H}{N_H}S_H\Psi_{I_H} + \alpha_H\Psi_{R_H}\right] \tag{48}$$

$$\frac{d\Psi_{S_P}}{dt} = -\frac{\partial H}{dS_P} = \left[\left((1-C_3)\xi_P\left(1-\frac{S_P}{N_P}\right)+\alpha_P\right)\Psi_{S_P} - \left((1-C_3)\xi_P\left(1-\frac{S_P}{N_P}\right)\right)\Psi_{I_P}\right] \tag{49}$$

$$\frac{d\Psi_{I_P}}{dt} = -\frac{\partial H}{dI_P} = \begin{bmatrix} -T^2 + \left((1-C_1)\frac{\lambda_P\phi_P-\xi_H}{N_H}\right)S_H\Psi_{S_H} - \left((1-C_1)\frac{\lambda_P\phi_P-\xi_H}{N_H}\right)S_H\Psi_{I_H} + \left((1-C_3)\frac{\lambda_P\phi_P-\xi_P}{N_P}\right)S_P\Psi_{S_P} \\ -\left((1-C_3)\frac{\lambda_P\phi_P-\xi_P}{N_P} - (C_4+\alpha_H+\beta_H)\right)S_P\Psi_{I_P} - C_4\Psi_{T_P} \end{bmatrix} \tag{50}$$

$$\frac{d\Psi_{T_P}}{dt} = -\frac{\partial H}{dT_P} = \left[-T^1 + \left((1-C_3)\frac{\xi_P}{N_P}\right)S_P\Psi_{S_P} - (1-C_3)\frac{\xi_P}{N_P}S_P\Psi_{I_P} + (\sigma_P+\alpha_P+\beta_P)\Psi_{T_P} - \sigma_P\Psi_{R_P}\right] \tag{51}$$

$$\frac{d\Psi_{R_P}}{dt} = -\frac{\partial H}{dR_P} = \left[\left((1-C_3)\frac{\xi_P}{N_P}\right)S_P\Psi_{S_P} - (1-C_3)\frac{\xi_P}{N_P}S_P\Psi_{I_P} + \alpha_P\Psi_{R_P}\right] \tag{52}$$

$$\frac{d\Psi_{S_B}}{dt} = -\frac{\partial H}{dS_B} = \left[\left(\xi_B\left(1-\frac{S_B}{N_B}\right)+\alpha_B\right)\Psi_{S_B} - \left(\xi_B\left(1-\frac{S_B}{N_B}\right)\right)\Psi_{I_B}\right] \tag{53}$$

$$\frac{d\Psi_{I_B}}{dt} = -\frac{\partial H}{dI_B} = \begin{bmatrix} \left((1-C_1)\frac{\lambda_B\phi_B-\xi_H}{N_H}\right)S_H\Psi_{S_H} - \left((1-C_1)\frac{\lambda_B\phi_B-\xi_H}{N_H}\right)S_H\Psi_{I_H} + \left((1-C_3)\frac{\lambda_B\phi_B-\xi_P}{N_P}\right)S_P\Psi_{S_P} \\ -\left((1-C_3)\frac{\lambda_B\phi_B-\xi_P}{N_P}\right)S_P\Psi_{I_P} + \left(\frac{\lambda_B\phi_B-\xi_B}{N_B}\right)S_B\Psi_{S_B} - \left(\frac{\lambda_B\phi_B-\xi_B}{N_B}\right)S_B\Psi_{I_B} + (\alpha_B+\beta_B)\Psi_{I_P} \end{bmatrix} \tag{54}$$

Given the conditions of transversally to be

$$\Psi_i, i \in \{S_H, I_H, T_H, R_H, S_P, I_P, T_P, R_P, S_B, I_B\}.$$

In pursuit of minimizing the Hamiltonian, denoted as H, in relation to the optimal control variables, we undertake the process of differentiation with respect to $C = C_1, C_2, C_3, C_4$. By doing so, we derive a set of equations, which we subsequently set to zero in order to solve for the optimal control configuration. This procedure yields the sought-after optimal control solution.

Taking $S_H = S_H^*, I_H = I_H^*, T_H = T_H^*, R_H = R_H^*, S_P = S_P^*, I_P = I_P^*, T_P = T_P^*, R_P = R_P^*, S_B = S_B^*, I_B = I_B^*$

$$\begin{aligned} \frac{dH}{dC_1} &= U_1C_1{}^* + \xi_H S_H\Psi_{S_H} - \xi_H S_H\Psi_{I_H} = 0 \\ \frac{dH}{dC_2} &= U_2C_2{}^* - I_H\Psi_{I_H} + I_H\Psi_{T_H} = 0 \\ \frac{dH}{dC_3} &= U_3C_3{}^* + \xi_P S_P\Psi_{S_P} - \xi_P S_P\Psi_{I_P} = 0 \\ \frac{dH}{dC_\$} &= U_4C_4{}^* - I_P\Psi_{I_P} + I_P\Psi_{T_P} = 0 \end{aligned} \tag{55}$$

By simplification, we obtain solution for the optimal control to be

$$C_1^* = \frac{\xi_H S_H \left(\Psi_{I_H} - \Psi_{S_H}\right)}{U_1}$$
$$C_2^* = \frac{I_H \left(\Psi_{I_H} - \Psi_{T_H}\right)}{U_2} \quad (56)$$
$$C_3^* = \frac{\xi_P S_P \left(\Psi_{I_P} - \Psi_{S_P}\right)}{U_1}$$
$$C_4^* = \frac{I_P \left(\Psi_{I_P} - \Psi_{T_P}\right)}{U_2}$$

Now, making use of the boundary conditions, the solution is given has

$$C_1^* = \min\{1, \max\{0, D_1\}\};$$
$$C_2^* = \min\{1, \max\{0, D_2\}\}; \quad (57)$$
$$C_3^* = \min\{1, \max\{0, D_3\}\},$$
$$C_4^* = \min\{1, \max\{0, D_4\}\};$$

Where,

$$D_1 = \frac{\xi_H S_H \left(\Psi_{I_H} - \Psi_{S_H}\right)}{U_1}; D_2 = \frac{I_H \left(\Psi_{I_H} - \Psi_{T_H}\right)}{U_2}; D_3 = \frac{\xi_P S_P \left(\Psi_{I_P} - \Psi_{S_P}\right)}{U_1}; D_4 = \frac{I_P \left(\Psi_{I_P} - \Psi_{T_P}\right)}{U_2} \quad (58)$$

Proved.

Numerical Solution

In this simulation, we offer a means to observe the progression of the disease over time, track alterations in various parameters, and evaluate the effectiveness of interventions. This platform enables researchers and public health authorities to acquire valuable insights into the disease's behavior across different scenarios and to assess the efficacy of diverse control tactics. The state variables' initial conditions are as follows:, $S_H = 200$, $I_H = 150$, $T_H = 140$, $R_H = 120$, $S_P = 250$, $I_P = 200$, $T_P = 190$, $R_P = 150$, $S_B = 150$ and $I_B = 140$. Also, ψ_H =20; ψ_P =4; ψ_B =2; σ_H =0.58; σ_P =0.01. The parameter values needed for the simulation are displayed in Table 3.

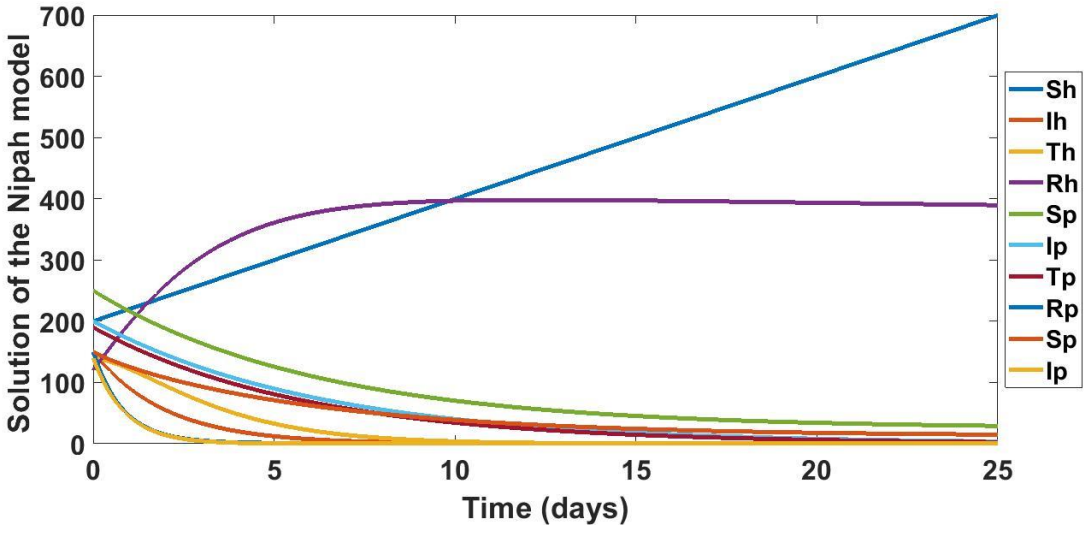

Figure 3: Trajectories solution of the Nipah model

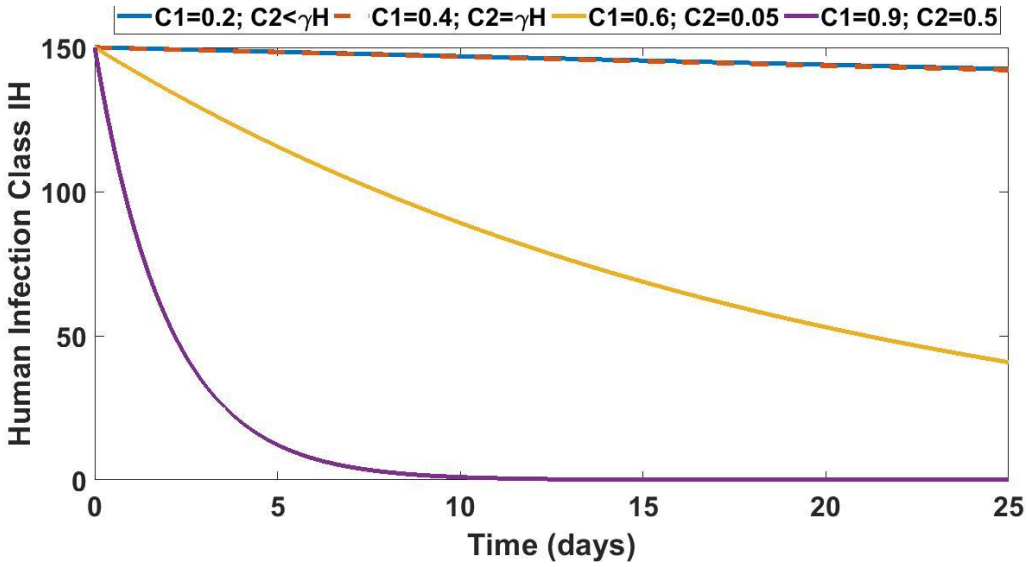

Figure 4: Trajectories solution for optimizing human infected class

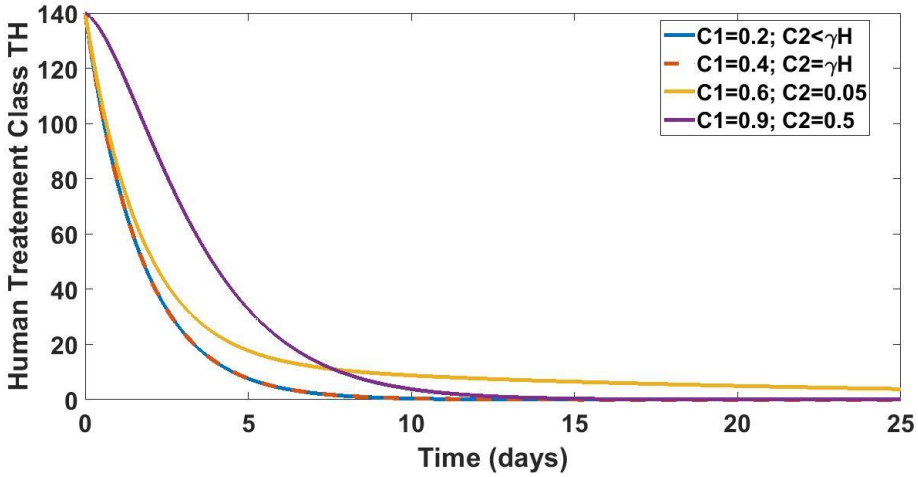

Figure 5: Trajectories solution for optimizing human treatment class

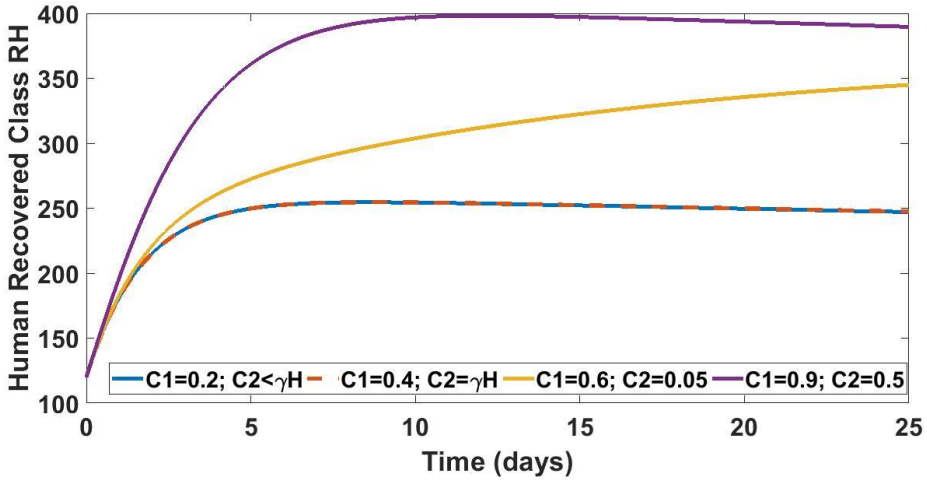

Figure 6: Trajectories solution for optimizing human recovered class

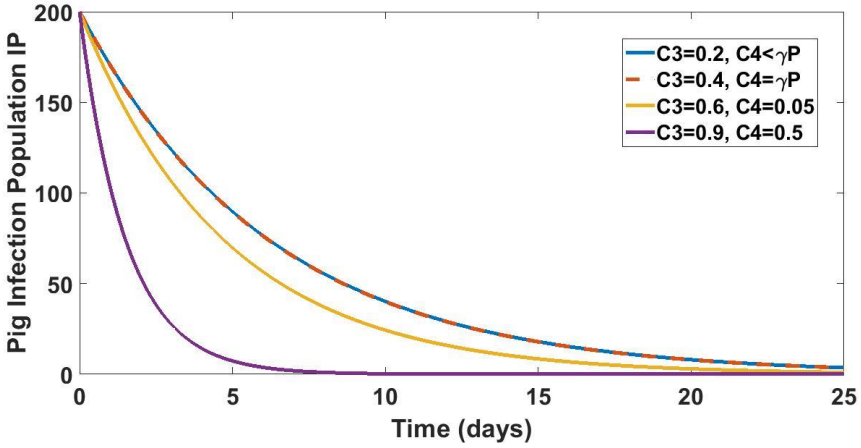

Figure 7: Trajectories solution for optimizing pig infection population

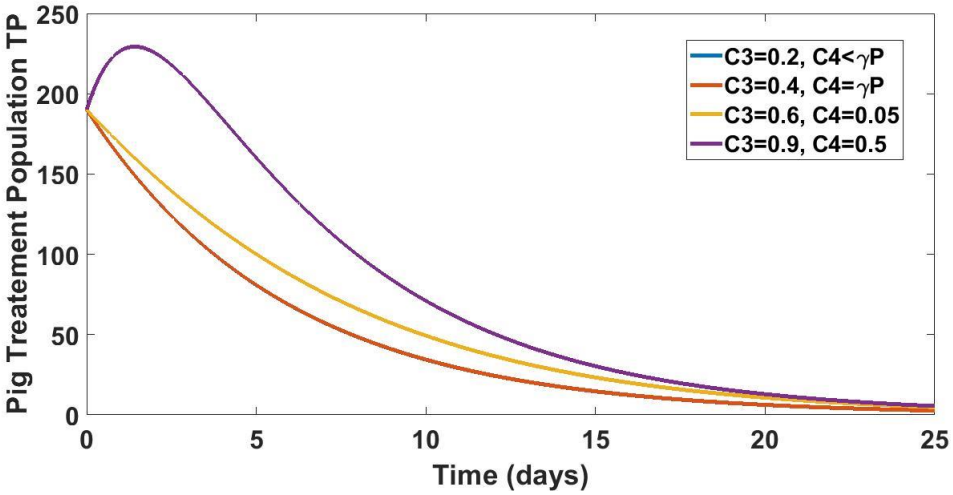

Figure 8: Trajectories solution for optimizing pig treatment population

RESULTS AND DISCUSSION

Figure 6 shows all the compartments of the Nipah virus model and this serves several important purposes in understanding and analyzing the dynamics of the Nipah virus transmission, also this enhances the model's explanatory power, aids in understanding Nipah virus transmission processes, and supports decision-making for control and prevention strategies.

The positive implications of the control measures implemented in the mathematical model of Nipah virus, as indicated by **Figure 7**, are noteworthy. These measures, which encompass personal prevention practices such as handwashing, avoidance of contact with sick birds or pigs, refraining from consuming potentially contaminated products, and minimizing contact with infected individuals, along with the treatment of infected individuals, have yielded a significant reduction in the human infection class compartment. This decline in human infections signifies the effectiveness of the control measures in curtailing the spread of the virus. It reflects a successful effort to mitigate the transmission of Nipah virus from its natural reservoirs, such as bats and intermediate hosts like pigs, to humans. The reduction in human infections is not only a testament to the positive impact of these control measures on public health but also an indication of the potential to prevent or manage outbreaks more effectively. By employing such strategies, we can enhance our capacity to safeguard communities from Nipah virus infections and, in turn, reduce the associated risks to human health and well-being.

The positive implication of the control measures depicted in **Figure 8** of the mathematical model of Nipah virus is the dynamic effectiveness of these measures in managing the outbreak. As the optimal control of human treatment class increases to a certain level, it indicates that a proactive approach to treating infected individuals is yielding positive results. This implies that access to medical care, isolation, and treatment for infected patients are contributing to their recovery and survival. The reduction in the human treatment class after reaching a certain level suggests that these control measures are successfully curbing the spread of the virus, leading to a decline in the number of individuals requiring treatment. This demonstrates the potential of early detection, improved healthcare, and the application of appropriate treatment in reducing the severity of Nipah virus infections and preventing further transmission. Ultimately, the dynamic nature of the model highlights the adaptability and effectiveness of these control measures in containing the outbreak and safeguarding public health.

In **Figure 9**, the observed increase in the human recovered class compartment as the optimal control measure is increased, specifically through personal prevention and treatment of infected individuals, carries several positive implications. Firstly, it signifies the effectiveness of these control measures in curbing the spread of the virus and aiding in the recovery of infected individuals. Personal prevention measures, such as handwashing and avoiding contact with sick birds or pigs, not only protect individuals from initial exposure but also break the chain of transmission, ultimately reducing the number of new infections. Secondly, the emphasis on the treatment of infected individuals is vital for improving their chances of recovery and survival. This leads to a higher proportion of individuals transitioning to the recovered class, indicating a positive outcome in terms of reducing the disease's impact. Overall, the observed increase in the human recovered class compartment highlights the success of these control measures in mitigating the Nipah virus's impact on human health and underscores the importance of continued efforts in their implementation and promotion.

The implication of the control measures, which include biosecurity measures and public health intervention as well as the effort of treating the pig population, is evident in **Figure 10**. As the optimal control is increased, leading to a reduction in the pig infection population compartment, several significant benefits are realized. First and foremost, this reduction in pig infections represents a lower risk of Nipah virus transmission from pigs to humans, thereby decreasing the potential for human infections. Moreover, it reflects the effectiveness of biosecurity measures and public health interventions in containing the spread of the virus in pig populations. This reduction not only safeguards public health but also has economic implications by preserving the pig farming industry. In summary, the decrease in pig infections signifies the success of these control measures in minimizing the risk of Nipah virus outbreaks, protecting both human health and the livelihood of pig farmers.

In **Figure 11**, the observed increase in the pig treatment population compartment from day 0 to day 15, followed by a reduction as optimal control measures are implemented, carries several positive implications. Firstly, it reflects the effectiveness of the biosecurity measures and public health interventions being put into action. This increase signifies that more pigs are receiving timely treatment and care, which is crucial in limiting the spread of the Nipah virus among the pig population. As these measures are scaled up, the subsequent reduction suggests that the virus's impact on the pig population is diminishing, which is a significant step in preventing the virus from reaching humans through the zoonotic pathway. Ultimately, this trend underlines the success of these control measures in safeguarding both animal and human health, emphasizing the importance of early intervention and comprehensive biosecurity practices in reducing the risk of Nipah virus transmission.

CONCLUSION

In conclusion, the comprehensive analysis of various compartments in the Nipah virus mathematical model, as illustrated in Figures 6 to 11, provides valuable insights into the dynamics of Nipah virus transmission. These visual representations enhance the model's explanatory power and aid in understanding the processes involved in Nipah virus transmission. The positive implications of the control measures, including personal

prevention practices, treatment of infected individuals, biosecurity measures, and public health interventions, are evident in the reduction of human and pig infections, as well as the increase in the pig treatment population. These outcomes underscore the effectiveness of these control strategies in mitigating the spread of the virus, protecting public health, and supporting the livelihood of pig farmers. Overall, these findings emphasize the importance of proactive measures in preventing and managing Nipah virus outbreaks, ultimately reducing the risks to human health and well-being.

ACKNOWLEDGEMENT

Mrs. Adetoun Loyinmi, Mr. Mathew and Mrs. Alice Gbodogbe are appreciated for their supports.

REFERENCES

[1]. World Health Organization. Fact sheet: Nipah virus *(https://www.who.int/news-room/fact-sheets/detail/nipah-virus)*. Last reviewed 5/2018. Accessed 6/20/2023.
[2]. Loyinmi, A.C. and Idowu, K.O. (2023). Semi –analytical approach to solving Rosenau-Hyman and Korteweg-de Vries equations using integral transform. *Tanzan J Sci*. 49:26-40. https://doi.org/10.4314/tjs.v49il.3.
[3]. Loyinmi, A.C. and Oredein, A.I. (2011). The unsteady variable viscosity free convection flow on a porous plate. *J. Niger. Assoc. Math. Phys.* 19: 229-232. https://www.ajol.info/index.php/jonamp/article/view/91459.
[4]. Agbomola, J. and Loyinmi, A. A. (2022). mathematical model for the dynamical behavior of Ebola transmission in human-bat population: implication of immediate discharge of recovered individuals. *Preprints*.
[5]. Banerjee, S., Gupta, N., Kodan, P., Mittal, A., Ray, Y., Nischal, N. et al. Nipah virus disease: A rare and intractable disease (https://www.ncbi.nlm.nih.gov/pmc/articles/PMC6409114/). Intractable Rare Dis Res. 2019 Feb;8(1):1-8. Accessed 6/20/2023.
[6]. Loyinmi, A.C., Oredein, A.I. and Prince S. U. (2018). Homotopy adomian decomposition method for solving linear and nonlinear partial differential equations. *Tasued J. Pure Appl. Sci*. 1: 254-260.
[7]. Agbomola, J.O. and Loyinmi, A.C. (2022). Modelling the impact of some control strategies on the transmission dynamics of Ebola virus in human-bat population: An optimal control analysis. *Heliyon*. 8:e12121. https://doi.org/10.1016/j.heliyon.2022.e12121.
[8]. Centers for Disease Control and Prevention (U.S.). What is Nipah Virus? *(https://www.cdc.gov/vhf/nipah/about/index.html)* Last reviewed 10/2022. Accessed 6/20/2023.
[9]. Loyinmi, A.C. and Lawal, O.W. (2011). The asymptotic solution for the steady variable-viscosity free convection flow on a porous plate. *J. Niger. Assoc. Math. Phys*. 19:273- 276.
[10]. Loyinmi, A.C., Lawal, O.W. and Sottin, D.O. (2017). Reduced differential transform method for solving partial integro-differential equation. *J. Niger. Assoc. Math. Phys*. 43: 37-42.
[11]. National Emerging Special Pathogens Training & Education Center. What You Need to Know about Nipah Virus *(https://netec.org/2023/02/10/what-you-need-to-know-about-nipah-virus/)*. Accessed 6/20/2023.
[12]. Loyinmi, A.C., Erinle-Ibrahim, L.M. and Adeyemi, A.E. (2017). The new iterative method (NIM) for solving telegraphic equation. *J. Niger. Assoc. Math. Phys*. 43: 31- 36.
[13]. Idowu, K.O., Akinwande, T.G., Fayemi, I., Adam, U.M. and Loyinmi, A.C. (2023). Laplace homotopy perturbation method (LHPM) for solving system of N-dimensional non-linear partial differential equation. *Al-Bahir Journal for Engineering and Pure Sciences*. 3(1): 11-27. https://doi.org.10.55810/2313-0083.1031.
[14]. Osmosis by Elsevier. Nipah Virus *(https://www.osmosis.org/answers/nipah-virus)*. Accessed 6/20/2023.
[15]. Akinfe, K.T. and Loyinmi, A.C. (2021). The implementation of an improved differential transform scheme on the Schrodinger equation governing wave-particle duality in quantum physics and optics. *Results in physics*. https://doi.org/10.1016/j.rinp.2022.105806.
[16]. Akinfe, T.K. and Loyinmi, A.C. (2022). An improved differential transform scheme implementation on the generalized Allen-Cahn equation governing oil pollution dynamics in oceanography. *Partial Differ. Equations Appl. Math*. 6:100416. https://doi.org/10.1016/j.padiff.2022.100416.
[17]. Akinfe, T.K. and Loyinmi, A.C. (2020). An algorithm for solving the Burgers-Huxley equation using the Elzaki transform. *SN Appl. Sci*.2: 1-17. https://doi.org/10.1007/s42452-019-1652-3.
[18]. American Society for Microbiology. What You Need to Know About Nipah Virus *(*https://asm.org/Articles/2023/April/What-You-Need-to-Know-About-Nipah-Virus*)* . Last reviewed 4/2023. Accessed 6/20/2023.

[19]. Akinfe, T.K.and Loyinmi, A.C. (2021). A solitary wave solution to the generalized Burgers-Fisher's equation using an improved differential transform method: a hybrid approach scheme approach. *Heliyon*. 7:e07001. https://doi.org/10.1016/j.heliyon.2021.e07001.

[20]. Loyinmi, A.C. and Akinfe, T.K. (2020). Exact solution to the family of Fisher's reaction-diffusion equations using Elzaki homotopy transformation perturbation method. *Eng. Reports*. 2:e12084. https://doi.org/10.1002/eng2.12084.

[21]. Akinfe, K.T. and Loyinmi, A.C. (2022). Stability analysis and semi-analytical solution to a SEIR-SEI Malaria transmission model using He's variational iteration method. *Preprints*.

[22]. Akinfe, K.T. (2023). A reliable analytic technique for the modified proto-typical Kelvin-Voigt viscoelastic fluid model by means of the hyperbolic tangent function. *Partial Differ. Equations Appl. Math*. 7:10523. https://doi.org/10.1016/j.padiff.2023.100523.

[23]. Idowu, K.O. and Loyinmi, A.C. (2023). The analytical solution of non-linear Burgers-Huxley equations using the Tanh method. *Al-Bahir journal for Engineering and Pure Sciences*. 3:1, 68-77. https://doi.ord/10.55810/2312-5721.1038.

[24]. Idowu, O.K. and Loyinmi, A.C. (2023). Qualitative analysis of the transmission dynamics and optimal control of covid-19. *EDUCATUM Journal of Science, Mathematics and Technology*. 10: 1, 54-70. https://doi.org/10.37134/ejsmt.vol10.1.7.2023.

[25]. Loyinmi, A.C., Akinfe, T.K. and Ojo, A.A. (2021). Qualitative analysis and dynamical behavior of a Lassa haemorrhagic fever model with exposed rodents and saturated incidence rate. *Sci. African*. 14; e01028. https://doi.org/10.1016/j.sciaf.2021.e01028.

[26]. Lawal, O.W., Loyinmi, A.C. and Erinle-Ibrahim, L.M. (2018). Algorithm for solving a generalized Hirota-Satsuma coupled KDV equation using homotopy perturbation transformed method. *Science World Journal*. 13: 23-28.

[27]. Lawal, O.W. and Loyinmi, A.C. (2019). Application of new iterative method for solving linear and nonlinear initial boundary value problems with non-local conditions. *Science World Journal*. 2019; 14: 100-104.

[28]. Lawal, O.W.; Loyinmi, A.C.; Sowumi, S.O. Homotopy perturbation algorithm using Laplace transform for linear and nonlinear ordinary delayed differential equation. *J. Niger. Assoc. Math. Phys*. 2017; 41:27- 34.

[29]. Lawal, O.W., Loyinmi, A.C. and Hassan, A.R. (2019). Finite difference solution for Magneto hydrodynamics thin film flow of a third grade fluid down inclined plane with ohmic heating. *J. Math. Assoc. Niger*. 46, 1: 92-97.

[30]. Lawal, O.W. and Loyinmi, A.C. (2017). Approximate solutions of higher dimensional linear and nonlinear initial boundary problems using new iterative method. *J. Niger. Assoc. Math. Phys*. 41:35- 40.

[31]. Lawal, O.W., Loyinmi, A.C. and Ayeni, O.B. (2019). Laplace homotopy perturbation method for solving coupled system of linear and nonlinear partial differential equation. *J. Math. Assoc. Niger*. 46, 1; 83-91.

[32]. Lawal, O.W. and Loyinmi, A.C. (2012). Magnetic and porosity effect on MHD flow of a dusty visco-elastic fluid through horizontal plates with heat transfer. *J. Niger. Assoc. Math. Phys*. 21: 95- 104.

[33]. Lawal, O.W. and Loyinmi, A.C. (2011). The effect of magnetic field on MHD viscoelastic flow and heat transfer over a stretching sheet. *Pioneer J. Adv. Appl. Math*. 3: 83-90.

[34]. Lawal, O.W. and Loyinmi, A.C. (2011). Oscillating flow on a visco-elastic fluid under exponential pressure gradient with heat transfer. *Pioneer J. Adv. Appl. Math*. 3: 33-82.

[35]. Idowu, K.O. and Loyinmi, A.C. (2023). Impact of contaminated surfaces on the transmission dynamics of corona virus disease (Covid-19). *Biomed J. Sci. Tech. Res*. 51: 42280-90. https://doi.org/10.26717/BJSTR 2023.51008046.

[36]. Erinle-Ibrahim, L.M., Adewole, A.I., Loyinmi, A.C. and Sodeinde, O.K. (2020). An optimization scheme using linear programming in a production line of rites food limited, Ososa. *FUDMA J. Sci*. 4: 502-510.

[37]. M. Biswas. (2012). Model and control strategy of the deadly nipah virus (niv) infections in Bangladesh. *Research & Reviews in Biosciences.* 6 (12), 370–377.

[38]. M. H. A. Biswas. (2014). Optimal control of nipah virus (niv) infections: a Bangladesh scenario. *Journal of Pure and Applied Mathematics: Advances and Applications*. 12 (1), 77–104.

[39]. M. H. A. Biswas., M. M. Haque. and G. Duvvuru. (2015). A mathematical model for understanding the spread of nipah fever epidemic in Bangladesh in 2015 International Conference on Industrial Engineering and Operations Management (IEOM), pp. 1–8, IEEE.

[40]. J. Sultana and C. N. Podder. (2016). Mathematical analysis of nipah virus infections using optimal control theory, *Journal of Applied Mathematics and Physics*. 4 (6), 1099–1111.

[41]. M. K. Mondal, M. Hanif, M. H. A. Biswas. (2017). A mathematical analysis for controlling the spread of Nipah virus infection. *International Journal of Modeling and Simulation*. 37 (3), 185–197.

[42]. N. H. Shah, A. H. Suthar, F. A. Thakkar and M. H. Satia. (2018). SEI-model for transmission of Nipah virus. *The Journal of Mathematics and Computer Science*. 8 (6), 714–730.

[43]. D. Sinha and A. Sinha. (2019). Mathematical model of zoonotic Nipah virus in south-east Asia region. *Acta Scientific Microbiology*. 2 (9), 82–89.

[44]. H. S. Nita, D. T. Niketa, A. T. Foram and H. S. Moksha. (2018). Control strategies for Nipah virus. *International Journal of Applied Engineering Research*. 13 (21), 15149–15163.

[45]. Van Doremalen, N., Lambe, T., Sebastian, S., Bushmaker, T., Fischer, R., Feldmann, F. and Munster, V. (2020). A single-dose ChAdOx1-vectored vaccine provides complete protection against Nipah Bangladesh and Malaysia in Syrian golden hamsters. *PLoS neglected tropical diseases*, *13*(6), e0007462.

[46]. Scott, A. S. I., Luke, O. A., William, A., Emeka, O. K., Adebisi, A. R., Nnamani, T. N. and Ezike, M. G. C. (2023). Mathematical modelling approach for the study of Nipah virus disease transmission dynamics. *Commun. Math. Biol. Neurosci.* Article-ID.

[47]. A.D. Zewdie and S. Gakkhar. (2020). A mathematical model for Nipah virus infection, *J. Appl. Math*. 6050834. https://doi.org/10.1155/2020/6050834.

[48]. R.K. Singh, K. Dhama, S. Chakraborty, et al. (2019). Nipah virus: epidemiology, pathology, immunobiology and advances in diagnosis, vaccine designing and control strategies - a comprehensive review, Vet. Quart. 39, 26-55. https://doi.org/10.1080/01652176.2019.1580827 .

[49]. S.K. Jain, S. Tyagi, N. Dhiman, et al. (2021). Study of dynamic behaviour of psychological stress during COVID-19 in India: *A mathematical approach*, *Results Phys*. 29, 104661. https://doi.org/10.1016/j.rinp.2021.10 4661.